HHS Public Access

Author manuscript

Curr Biol. Author manuscript; available in PMC 2022 October 25.

Published in final edited form as:

Curr Biol. 2021 October 25; 31(20): 4449–4461.e4. doi:10.1016/j.cub.2021.07.069.

Sex-specific, *pdfr-1*-dependent modulation of pheromone avoidance by food abundance enables flexibility in *C. elegans* foraging behavior

Jintao Luo, **Douglas S. Portman***

Department of Biomedical Genetics, Del Monte Institute for Neuroscience, University of Rochester School of Medicine and Dentistry, Rochester, NY 14642

SUMMARY

To make adaptive feeding and foraging decisions, animals must integrate diverse sensory streams with multiple dimensions of internal state. In *C. elegans*, foraging and dispersal behaviors are influenced by food abundance, population density, and biological sex, but the neural and genetic mechanisms that integrate these signals are poorly understood. Here, by systematically varying food abundance, we find that chronic avoidance of the population-density pheromone ascr#3 is modulated by food thickness, such that hermaphrodites avoid ascr#3 only when food is scarce. The integration of food and pheromone signals requires the conserved neuropeptide receptor PDFR-1, as *pdfr-1* mutant hermaphrodites display strong ascr#3 avoidance even when food is abundant. Conversely, increasing PDFR-1 signaling inhibits ascr#3 aversion when food is sparse, indicating that this signal encodes information about food abundance. In both wild-type and *pdfr-1* hermaphrodites, chronic ascr#3 avoidance requires the ASI sensory neurons. In contrast, PDFR-1 acts in interneurons, suggesting that it modulates processing of the ascr#3 signal. Although a sex-shared mechanism mediates ascr#3 avoidance, food thickness modulates this behavior only in hermaphrodites, indicating that PDFR-1 signaling has distinct functions in the two sexes. Supporting the idea that this mechanism modulates foraging behavior, ascr#3 promotes ASI-dependent dispersal of hermaphrodites from food, an effect that is markedly enhanced when food is scarce. Together, these findings identify a neurogenetic mechanism that sex-specifically integrates population and food abundance, two important dimensions of environmental quality, to optimize foraging decisions. Further, they suggest that modulation of attention to sensory signals could be an ancient, conserved function of *pdfr-1*.

Graphical Abstract

* Corresponding Author and Lead Contact: douglas.portman@rochester.edu, Twitter: @doug_p, @portmanlab.

AUTHOR CONTRIBUTIONS

Conceptualization: J.L. and D.P.; Investigation: J.L.; Writing — Original Draft: J.L.; Writing — Review & Editing: D.P.; Supervision: D.P.; Funding Acquisition: D.P.

DECLARATION OF INTERESTS

The authors declare no competing interests.

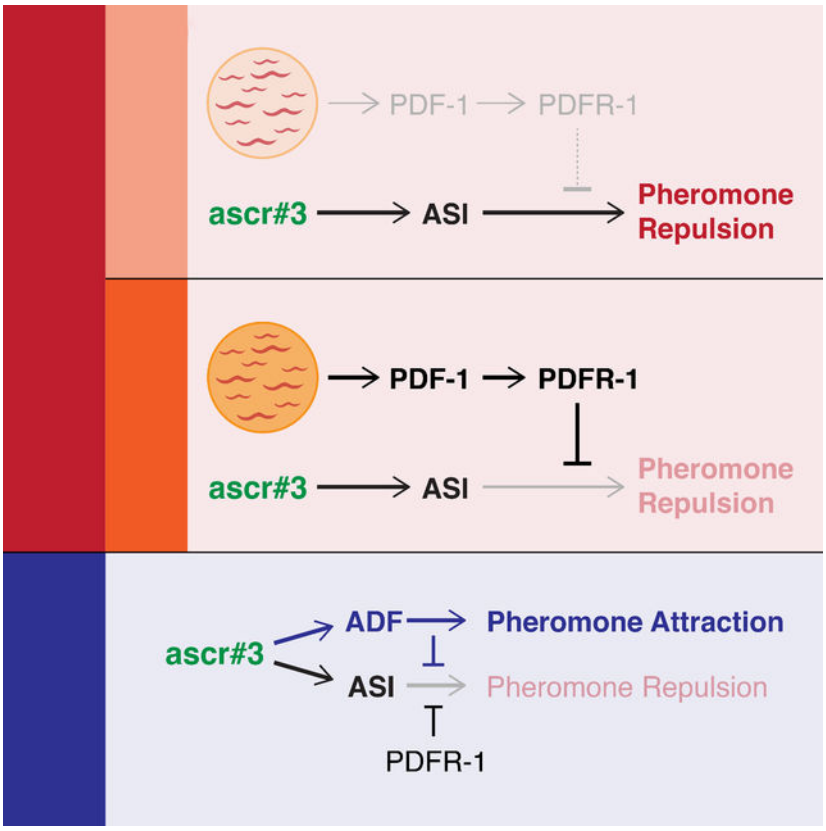

eTOC Blurb

To forage optimally, animals must predict the future value of an existing food resource. Here, Luo and Portman show that *C. elegans* can assess this by weighing food abundance against population density. The authors find that food abundance engages a conserved neuromodulatory pathway to modulate avoidance of a key population density pheromone.

INTRODUCTION

Feeding and foraging provide ideal opportunities to understand the neural and genetic mechanisms underlying flexibility in innate behavior. Despite wide variation in the mechanics of foraging, the logic that guides decisions about exploiting or abandoning food resources is remarkably conserved. In animals as diverse as bees, birds, and fish, foraging decisions weigh the current benefit of feeding against the costs of exploration and the potential benefits of new food sources [1,2]. When assessing the value of an existing food resource, optimal foraging requires that animals assess local food abundance and quality as well as population density, nutritional needs, and the risk of predation. Experimental studies have provided important insights into the neural mechanisms underlying these calculations and the genetic mechanisms that specify and optimize them [3].

The nematode *C. elegans* feeds on microbes that colonize decaying vegetation [4] and modulates its feeding and exploratory behaviors in ways that are consistent with optimal foraging theory. Foraging and dispersal in adults varies with food abundance [5,6], nutritional

value [7,8], pathogenicity and toxicity [9,10], and experience [11,12]. Foraging behavior exhibits substantial natural variation, owing in part to altered sensory responses [6,13–17]. Furthermore, foraging and dispersal are sexually dimorphic and sensitive to nutritional state: solitary males will abandon a food source in search of mates, but only if well-fed [18–22].

In many species, foraging is sensitive to population density. Conspecifics can be competitors that reduce the future value of a crowded food source, but in other contexts, collective foraging can be advantageous [23]. In *C. elegans*, worms will leave a food source more often if it is crowded [17,24], but some pheromones inhibit dispersal and exploration [6,15,16]. Further, many natural isolates feed in groups [13] and collective foraging may be favored in patchy food environments [25,26]. Thus, the role of population density in *C. elegans* foraging and dispersal may not be fixed. Indeed, in the wild, balancing selection can simultaneously maintain alleles that promote both strategies [16,17].

Because of its “boom-and-bust” life cycle, in which food availability and population density can vary dramatically [27], *C. elegans* actively monitor both of these variables when feeding. Population density in *C. elegans* is mainly signaled by ascarosides, derivatives of the dideoxy sugar ascarylose that serve as a modular chemical language [28–30]. A prominent member of this group is ascr#3, which, together with other ascarosides, signals population density to young larvae, guiding the decision to enter the stress-induced dauer stage [31,32]. ascr#3 is also a sex pheromone: it is produced predominantly by adult hermaphrodites and elicits strong male-specific attraction [33–35]. Adult hermaphrodite behavioral responses to ascr#3 are typically aversive, though this depends on the context of ascr#3 presentation as well as animals’ internal state and previous experience [26,33,35–39].

In earlier studies on sexual dimorphism [34], we encountered variability in hermaphrodite ascr#3 avoidance responses, leading us to wonder whether flexible responses to this population density signal might have adaptive value. Here, we find that this is the case, identifying a neuronal and genetic mechanism whereby food abundance modulates ascr#3 aversion specifically in hermaphrodites to adaptively modulate feeding and foraging decisions.

RESULTS

Hermaphrodite pheromone avoidance is modulated by food abundance

To explore the relationship between food and pheromones, we used a quadrant-format assay [34] (Figure 1A). This assay allows robust quantitation of medium-term (1–2 hr) behavioral responses to non-volatile chemical stimuli. To control the abundance of food, we prepared standardized lawns of *E. coli* OP50 of three densities (Figure 1B). “T3” is a smooth, uniform lawn providing ample but not excessive food, similar to standard culture conditions. “T2” is a thin, slightly patchy lawn. “T1” is a very thin lawn with many food-free patches, providing a scarce-food environment. Notably, other factors (e.g., bacterial metabolites and environmental gases) also likely differ between these conditions.

In hermaphrodites assayed with thin-food conditions (Figure 1C and S1), we observed modest but consistent avoidance of 1–5 μM ascr#3, but no response to lower concentrations

(0.1 and 0.01 μM). In males, 1–5 μM ascr#3 elicited robust attraction, but lower concentrations (0.01 μM and 0.1 μM) had little or no effect on behavior (Figure 1C). Thus, as expected, hermaphrodites and males on sparse food exhibit concentration-dependent, qualitatively distinct responses to ascr#3.

Surprisingly, when we assayed hermaphrodite behavior in the presence of thicker T3 food, we found that ascr#3 avoidance was absent (Figure 1D). Adult males, in contrast, displayed robust ascr#3 attraction regardless of food thickness (Figure 1D). This modulation of ascr#3 aversion by food abundance could reflect active integration of food and pheromone signals by the hermaphrodite nervous system; alternatively, thick food might simply block ascr#3 detection or response. We found that more concentrated ascr#3 (5 μM) was sufficient to elicit avoidance on thick food (Figure 1E), suggesting that the nervous system actively integrates these signals.

PDF neuropeptide signaling modulates pheromone avoidance

Because the conserved neuropeptide receptor PDFR-1 [40] is associated with both food-dependent and sex-specific behavioral states [19,41], we examined ascr#3 responses in *pdfr-1* null mutants. Interestingly, on thin food, *pdfr-1* hermaphrodites displayed markedly enhanced ascr#3 avoidance (Figure 2A, S2A). Single null mutations in *pdf-1* and *pdf-2*, which encode ligands for PDFR-1 [40], caused little change in ascr#3 avoidance. However, *pdf-1; pdf-2* double mutants showed strong avoidance (Figure 2A), suggesting functional redundancy. We detected no significant difference in ascr#3 avoidance between *pdfr-1* and *pdf-1; pdf-2* mutants, but cannot rule out possible signaling by additional PDFR-1 ligands or ligand-independent basal PDFR-1 signaling.

Because larval exposure to ascr#3 can alter adult ascr#3 responses [38], our results might point to a role for *pdfr-1* in experience-dependent plasticity. However, ascr#3 avoidance measured by the quadrant assay was independent of larval exposure to endogenously produced ascr#3, as the loss of *daf-22*, an enzyme necessary for synthesis of ascr#3 and other short-chain ascarosides [42], had no effect on aversion to exogenous ascr#3 in this context (Figure S2B).

PDFR-1 signaling intensity likely encodes food thickness information

Interestingly, we found that the ascr#3 responses of *pdfr-1* mutants were insensitive to food thickness. Regardless of food abundance, *pdfr-1* hermaphrodites showed strong aversion to ascr#3 (Figure 2B). This indicates that *pdfr-1* function is necessary for the integration of food-thickness information into hermaphrodite behavioral responses to ascr#3.

Because the neuropeptide receptor *npr-1* also modulates ascr#3 responses [35,36], we asked whether it might also have a role in this integration. On thin food, loss of *npr-1* had no apparent effect on ascr#3 avoidance. Moreover, *npr-1* mutants remained sensitive to food abundance, as ascr#3 avoidance was significantly blunted in the presence of thick food (Figure 2B). However, ascr#3 avoidance was not completely absent in *npr-1* mutants on thick food, suggesting that *npr-1* might have a role in the suppression of ascr#3 avoidance. Compared to *pdfr-1*, however, this role is subtle.

Consistent with the requirement for *pdfr-1*, ascr#3 avoidance was insensitive to food abundance in *pdf-1; pdf-2* double mutants (Figure 2C). Surprisingly, food-dependence was also absent in *pdf-1* single mutants but remained intact in *pdf-2* mutants (Figures 2D, E). Thus, although ligands encoded by both genes appear to have roles in the modulation of ascr#3 aversion, *pdf-1* has the primary role in linking food thickness to the strength of the aversive response.

We noted that the inhibitory function of *pdfr-1* appeared to be stronger on thick food than on thin food (Figure 2B), suggesting that the intensity of PDFR-1 signaling might encode information about food thickness. To test this, we asked whether artificially increasing *pdfr-1* signaling would block ascr#3 avoidance on thin food. To bring this about, we used transgenes carrying extra copies of wild-type *pdf-1* or *pdf-2* [40]. Consistent with our hypothesis, *pdf-1* overexpression reduced ascr#3 avoidance on thin food (Figures 2F, G). However, overexpression of *pdf-2* had no apparent effect (Figure 2F), again suggesting that *pdf-1*, but likely not *pdf-2*, conveys food thickness information. In agreement with this, overexpression of *pdf-1* had no apparent effect in the presence of thick food (Figure 2G). As expected, *pdfr-1* was required for the effect of *pdf-1* overexpression (Figure 2G). These results indicate that the intensity of PDFR-1 signaling, driven primarily by *pdf-1* activity, provides an instructive internal representation of food thickness that modulates ascr#3 avoidance.

The ASI sensory neurons are an essential component of the ascr#3 avoidance circuit

Next, we sought to characterize the neuronal basis for ascr#3 avoidance. In the absence of food, acute aversive and attractive responses to ascr#3 are mediated by the sensory neurons ADL and ASK, respectively [33,35,36,43]. However, genetic ablation of these neurons had no apparent effect on ascr#3 avoidance in the quadrant assay, either in wild-type or *pdfr-1* hermaphrodites (Figures 3A, B). Thus, the longer-term, on-food ascr#3 responses examined here are likely mediated by mechanisms distinct from those previously described.

We also considered the ASI neurons, which detect ascarosides in other contexts, including the dauer-entry decision [44] and the response to the exploration-suppressing pheromone icas#9 [16,45]. We found that ascr#3 avoidance was abolished upon ASI ablation, both in wild-type and *pdfr-1* backgrounds (Figures 3C), regardless of food thickness (Figures 3D, E). The requirement for ASI in both wild-type and *pdfr-1* mutants indicates that the strong ascr#3 avoidance of *pdfr-1* mutants likely results from increased activity of the same mechanism that generates avoidance in wild-type hermaphrodites, rather than the activation of a parallel mechanism.

These results suggested that ASI might directly detect ascr#3. However, using validated GCaMP transgenes and a range of pheromone concentrations, others have detected no evidence of ascr#3-evoked calcium responses in ASI (E. DiLoreto and J. Srinivasan, pers. comm.; K. Kim and P. Sengupta, pers. comm.). This is consistent with previous findings that ascarosides can engage signaling mechanisms over longer timescales without triggering calcium transients [15,32,45]. The simplest interpretation of our results is that ASI directly detects ascr#3; however, it is also possible that ASI is required downstream of ascr#3 detection or in parallel with it.

We also considered the possibility that ASI detects or implements the thin-food state, since ASI-ablated hermaphrodites mimic thick-food behavior (*i.e.*, indifference to ascr#3) on thin food (Figures 3C, D). However, this appeared not to be the case, as ASI ablation in *pdfr-1* mutants did not recapitulate the moderate ascr#3 repulsion typical of *pdfr-1* hermaphrodites on thick food (Figures 3C, E).

Because it is produced primarily by ASI, we also examined the TGFβ-superfamily ligand DAF-7 [46,47]. Like ASI-ablated hermaphrodites, *daf-7* hermaphrodites exhibited no net response to ascr#3 under any conditions (Figure 3F). We also tested *pdfr-1*; *daf-7* double mutants but observed exceptionally high variability in ascr#3 responses, suggesting a dysregulation of behavior in these animals. These results, which should be interpreted cautiously, could suggest a general requirement for *daf-7* in hermaphrodite ascr#3 avoidance. If so, *daf-7* might have a role in ascr#3 detection or might signal the presence or abundance of food (see Discussion).

PDFR-1 functions in multiple interneurons to modulate ascr#3 avoidance

pdfr-1 is expressed in multiple head and tail neurons, as well as peripheral tissues including body-wall muscle [19,40,48]. Using an established intersectional strategy [41], we tested the ability of a conditionally activatable *Ppdfr-1::inv[pdfr-1::SL2::gfp]* transgene, together with neuron-specific nCre constructs, to rescue the enhanced ascr#3 avoidance of *pdfr-1* hermaphrodites. This transgene produces functional *pdfr-1* and *GFP* only if the *Ppdfr-1* promoter is active and nCre-mediated recombination has taken place (Figure 4A).

Pan-neural nCre expression completely rescued the *pdfr-1* defect, while muscle expression had no effect (Figures 4B, C). Next, we tested a three-transgene combination ("*tmg::nCre*," driven by *Ptdc-1*, *Pmod-1*, and *Pglr-3*) previously shown to partially rescue the persistent dwelling of *pdfr-1* mutants [41]. However, we observed no rescue of ascr#3 avoidance with this transgene (Figure 4D). To ask whether *pdfr-1* functions in sensory neurons, we used *Posm-6::nCre*, but again saw no rescuing activity (Figure 4E). This suggests that *pdfr-1* is unlikely to function in ASI. Consistent with this, no GFP was detectable in animals carrying the ASI/AWA-specific *Pgpa-4::nCre* and the conditional *pdfr-1* transgene (not shown).

We generated and tested several other nCre constructs in combination with the conditional *pdfr-1* transgene. These strains exhibited no detectable GFP (*Pmec-10,* touch neurons) or failed to rescue the ascr#3 avoidance phenotype (*Pmod-1 + Posm-6,* GFP in several sensory neurons and interneurons; *Ptdc-1 + Pglr-3 + Pnmr-1,* GFP in many interneurons; and *Pgcy-28.d,* GFP in AIA interneurons) (not shown). (Note that we cannot rule out the possibility of weak, undetected rescue in these experiments.) However, with another combination, *Pgcy-28.d::nCre + Pnmr-1::nCre*, we observed a small but statistically significant reduction of ascr#3 avoidance in two independent transgenic lines (Figure 4F). To determine whether these effects were biologically meaningful, we assayed these lines with thick food, again observing significant rescuing activity (Figure 4G). In these animals, GFP was detected in several interneurons, including AIA, PVC, and one or more *nmr-1*-expressing head interneurons (AVA, AVD, AVE, AVG, and RIM). This partial rescue indicates that *pdfr-1* likely has additional important sites of action outside this subset of

neurons. From these results, we conclude that PDFR-1 has a distributed role in which it modulates multiple interneuronal components of the ascr#3 avoidance circuit.

The modulatory effects of food thickness are sex-specific

In males, sex-specific detection of ascr#3 by the ADF neurons promotes attraction in the quadrant assay [34]. Loss of *pdfr-1* or ASI had no effect on this behavior (Figures 5A, B), indicating that they are dispensable for male ascr#3 attraction.

When ADF is genetically feminized or ablated, males display hermaphrodite-like aversive responses to ascr#3, indicating that an avoidance mechanism is unmasked [34] (Figure 5C). Simultaneous ablation of ADF and ASI ablation eliminated all response to ascr#3 in males (Figure 5C), suggesting that avoidance is mediated by a mechanism common to both sexes. Supporting this, loss of *pdfr-1* enhanced the ascr#3 avoidance of ADF-ablated males, and this enhanced avoidance also required ASI (Figure 5D).

However, the behavior of ADF-ablated males was not completely equivalent to that of hermaphrodites. In particular, even in the presence of thick food, ADF-ablated males continued to manifest clear ascr#3 aversion (Figure 5E). We observed no effect of food thickness on ascr#3 attraction in *pdfr-1* males or on ascr#3 aversion in ADF-ablated *pdfr-1* males (Figures 5F, G). Thus, under these conditions, the modulation of ascr#3 avoidance by food thickness is a hermaphrodite-specific feature of the nervous system.

To investigate this sex difference, we genetically masculinized the hermaphrodite nervous system by pan-neuronal expression of the male sexual regulator *fem-3* [49]. This has been shown to functionally sex-reverse many behaviors mediated by shared circuits, including chemosensation and locomotion [22,34,50–52]. Simultaneously, we genetically ablated ADF to prevent it from driving ascr#3 attraction [34]. Interestingly, the modulatory effects of food thickness remained intact: thick food eliminated ascr#3 aversion in masculinized hermaphrodites, just as in WT (Figure 5H). Thus, sex-specific neurons and/or non-neuronal tissues, rather than sex-shared neurons, appear to be responsible for the hermaphrodite-specificity of food-pheromone integration.

Foraging decisions that integrate food abundance and population density cues require ASI

Finally, we wondered whether plasticity in ascr#3 avoidance might allow hermaphrodites to incorporate population density into their assessment of the value of an existing food resource. To explore this, we examined the dispersal of wild-type and ASI-ablated hermaphrodites from food sources of variable quality. In this assay, a thin (T1) or thick (T3) food source, supplemented with vehicle control or 1 μM ascr#3, lies at the center of a 10-cm agar plate (Figure 6A). Four peripheral patches of thick food without ascr#3, providing favorable alternative environments, lie 1.8 cm from the source patch. At the beginning of the assay, 50 young adult hermaphrodites (25 wild-type and 25 ASI-ablated, distinguishable by a fluorescent marker) were deposited on the source patch. After 3 hr, we scored the number of animals of each genotype that had migrated to the peripheral lawns.

When the source was a patch of thin food, relatively few animals migrated away, regardless of ASI ablation (Figure 6B). Supplementing the source patch with ascr#3 markedly

increased dispersal rate, with nearly 50% of animals migrating to the outer patches (Figure 6B). When ASI was ablated, however, addition of ascr#3 did not increase dispersal rates above baseline (Figure 6B). Thus, consistent with our findings in the quadrant assay, ascr#3 serves as a potent driver of dispersal when food is scarce, and this effect requires ASI.

With a thick-food source, we again observed relatively few animals dispersing (Figure 6B). Adding ascr#3 caused an increase in dispersal, but the magnitude of this effect was far smaller than with thin food (Figure 6B). Again, ascr#3-mediated dispersal was dependent on ASI. Thus, even on thick food, ascr#3 can have aversive effects; however, its ability to promote dispersal is markedly blunted.

Together, these results show that flexibility in ascr#3 aversion allows hermaphrodites to modulate foraging decisions according to population density and food abundance. The ASI-dependence of this plasticity strongly suggests that it arises through the same mechanism that modulates ascr#3 aversion in the quadrant assay. Because it provides a means for animals to optimize foraging decisions, this mechanism likely has adaptive value in the wild.

DISCUSSION

In making foraging decisions, animals weigh the future value of an existing food resource against the potential risks and benefits of abandoning it. A food resource's value depends not only on its quality and size, but also its projected rate of depletion, a primary determinant of which is local population density. How these variables are internally represented and used by neural circuits to calculate behavioral outcomes is poorly understood. Here, we show that *C. elegans* hermaphrodites dynamically assign a weight to the aversive population density signal ascr#3 based on food abundance, such that the salience of population density increases as food abundance diminishes (Figure 6C). This flexibility could allow hermaphrodites to disperse from a crowded, rapidly depleting food source before it is completely exhausted, avoiding potential starvation. When food is abundant, however, suppression of the population density signal could allow animals to continue to exploit an existing resource (Figure 6D). By identifying neural and genetic mediators of this process, our results provide insight into the neural mechanisms that implement behavioral plasticity and the genetically specified rules by which these mechanisms operate.

Our work builds on several studies showing that *C. elegans* hermaphrodites actively modulate their dispersal from an existing food resource [5,6,14,16,17,24,26]. Interestingly, recent work found that adult *C. elegans* hermaphrodites tend to increase food-leaving behavior as their self-progeny accumulate, and that this is likely a response to *daf-22*-dependent ascaroside pheromones produced by L1 larvae [24]. Our results indicate that the depletion of food might enhance this pheromone aversion, such that the larval-adult social interaction identified by these investigators could reflect a synergistic effect of abundant pheromone and scarce food. Another recent study provided evidence that dynamic modulation of the valence of ascaroside cues (i.e., repulsion vs. attraction) can optimize the foraging strategies of a population in a patchy food environment [26]. The relationship of these processes to the ascr#3 avoidance plasticity we report here will be an interesting area for future work.

Our findings indicate hermaphrodites use two distinct sensory streams to carry pheromone and food information (Figure 6C). For the former, the ASI sensory neuron pair plays a key role. While there is no evidence that ASI exhibits a calcium response to ascr#3 stimulation, we favor the possibility that ASI directly detects ascr#3 in the behavioral paradigm employed here. Indeed, previous work indicates that several classes of *C. elegans* sensory neurons including ASI can detect ascaroside pheromones directly without displaying a calcium transient [15,32,45]. Interestingly, these responses seem to act over a longer timescale than typical calcium-based neuronal signals, suggesting that they mediate "primer" effects of pheromones [16]. However, it is also possible that ASI function is required for the effects of an ascr#3 signal from other sensory neuron(s); these possibilities are not mutually exclusive. Our results also suggest that ASI's function depends on the TGFβ-superfamily signal DAF-7 (see below) [46,47]. Interestingly, ascr#3 detection mechanisms appear to be highly context-dependent, as the behaviors elicited by ascr#3 in other settings (*e.g.*, the acute drop test) have distinct neuronal substrates [33,35,36].

In our model, food abundance is signaled via a separate, parallel sensory stream (Figure 6C). Though the means by which food abundance is detected remain unclear, our findings strongly suggest that this variable is internally represented by the activity level of the neuropeptide receptor PDFR-1. Multiple lines of evidence support this. Animals lacking *pdfr-1* or the two ligand genes *pdf-1* and *pdf-2* display constitutively strong ascr#3 aversion that requires ASI but is completely insensitive to food thickness. Because this aversion is stronger than that seen in WT animals under thin-food (T1) conditions, we infer that low levels of PDFR-1 signaling are active when animals are on thin food, slightly blunting ascr#3 aversion. On thick food (T3), *pdfr-1* and *pdf-1; pdf-2* hermaphrodites still strongly avoid ascr#3, even though wild-type hermaphrodites are essentially indifferent to it. Here, high levels of PDFR-1 signaling completely inhibit ascr#3 aversion. Our results are most consistent with the idea that *pdf-1* and *pdf-2* have partially redundant functions but that *pdf-1*-derived ligand(s) have a more important role in signaling food thickness. Such partial redundancy also exists in other contexts [53], but several studies have shown that *pdf-2* can also antagonize *pdf-1* [40,54], indicating that the dynamics of this system are complex. Importantly, overexpressing *pdf-1* in animals feeding on thin food is sufficient to cause them to behave as though they were on thick food—that is, they are now indifferent to ascr#3—while overexpressing of *pdf-1* in animals feeding on thick food has no effect. Recently, *pdf-2* has been implicated in signaling nutritional status information from the intestine [55], raising the intriguing possibility that *pdf-1* and *pdf-2* communicate external and internal information about nutrition, respectively, to *pdfr-1*.

How might food abundance regulate *pdfr-1* signaling? We propose that the secretion of *pdf-1*-encoded neuropeptide(s) is regulated by a food thickness signal. Since sensory neurons are not a major site of *pdf-1* expression [48,56], sensory signals might be linked to *pdf-1* indirectly. One possibility is that *daf-7* conveys food abundance information to *pdf-1*. *daf-7* expression is responsive to food [46,47] and it can link food abundance to behavior, aging, and germline progenitor proliferation [57–59]. However, *daf-7* activity is expected to be low under thin-food conditions, where we see its strongest requirement [46,47] (Figure 3F). On thick food, where *daf-7* activity should be stronger, *daf-7* is not required for ascr#3 inhibition (Figure 3F). Thus, it is unlikely that *daf-7* conveys food

thickness information to the ascr#3 avoidance circuit. Instead, *daf-7* could have a permissive role, simply signaling the presence of food to enable pheromone avoidance. Alternatively, because *daf-7* is regulated by ascarosides in the dauer entry decision [46,47], *daf-7* might signal ascr#3 detection by ASI. However, *daf-7* is downregulated by ascaroside exposure [46,47], which would be problematic for such a model. Understanding the role of *daf-7* in ascr#3 avoidance will be an important area for future work.

At least four other previously identified mechanisms might couple food abundance to *pdf-1* activity. The physical presence of bacteria can be detected by the deirid sensory neuron ADE [60]; dopamine released by this neuron might in turn regulate PDF-1 secretion. Bacterial food is also a rich source of chemical cues [61]; the detection of these by amphid chemosensory neurons could indirectly regulate *pdf-1*. Further, in bacteria-rich environments, local concentrations of O_2 and CO_2 are decreased and increased, respectively, allowing worms to use the activity of gas-sensing neurons as proxies for food abundance [62–66]. *pdf-1* signaling could be downstream of such a signal. A final possibility is related to the physical structure of the sparse-food T1 environment, where bacterial patches are interspersed with many small gaps. As animals navigate this environment, the frequency with which they cross food boundaries is markedly higher than in an abundant-food environment. Recent work has shown that worms can use this information to assess the physical structure of food patches [12]; an intriguing possibility is that this might occur at least in part via modulation of PDF-1 release and/or PDFR-1 signaling.

Downstream of its regulation by food abundance, we find that PDFR-1 signaling represses ascr#3 aversion by modulating a distributed set of interneurons. *pdfr-1* is known to modulate the balance between roaming and dwelling states, another behavior affected by food quantity [8,41]. However, restoring *pdfr-1* function to neurons that mediate these effects was unable to rescue the increased ascr#3 aversion of *pdfr-1* mutants, suggesting that these are distinct functions. Future work will be required to understand how *pdfr-1* modulates the ascr#3 aversion circuit downstream of ASI.

Interestingly, biological sex regulates the processes we describe here in at least two ways. First, as shown previously, males-specific ascr#3 detection by ADF overrides a latent aversion drive [34]. Here, we show that this aversion appears to be mediated by a sex-shared mechanism, as it requires ASI and is repressed by *pdfr-1* in both sexes. However, the aversion driven by this mechanism is insensitive to food thickness: even in the presence of thick food, ADF-ablated males displayed ASI-dependent avoidance of ascr#3. Thus, some aspect of the food thickness signal—either its existence or its ability to modulate the aversive signal—is hermaphrodite-specific. Interestingly, this hermaphrodite-specific feature was not eliminated by genetic masculinization of the hermaphrodite nervous system. This suggests that the sex-specificity of food-pheromone integration depends on sex-specific neurons or sex-specific signals from peripheral tissues. Further, why males lack this sensory integration is unclear. One possibility is that, rather than encoding food thickness, *pdfr-1* signaling conveys some other dimension of information in males. The importance of *pdfr-1* in promoting male mate-searching behavior [19,67] strongly supports this idea.

Because of these differences, the scenarios of Figure 6D apply only to hermaphrodites. In males, ascr#3 would likely retain males under most of the conditions shown. This helps tune behavior to the distinct goals of adult males, in which mate-searching is typically favored over feeding [18,68]. Nevertheless, it seems unlikely that pheromone attraction in males is completely independent of food signals. In the absence of food, males copulate infrequently and poorly; both detection and ingestion of food are important for promoting efficient mating [69,70]. How males might integrate food and pheromone cues will be an interesting area for future research.

Neuromodulation is an ancient, widespread feature allowing the dynamic reconfiguration of fixed neural circuits [71]. Even in simple nervous systems, myriad neuromodulatory signals exist: the *C. elegans* genome, for example, contains over 100 neuropeptide genes, each of which can produce multiple ligands [72] (worm.peptidegpcr.org). While important progress has been made in identifying the effects of these signals on physiology and behavior, understanding the functional significance of the modulation they bring about can be challenging. Here, we provide evidence that PDF-1/PDFR-1 signaling is an internal representation of food abundance that regulates the behavioral response to stimulation by ascr#3. Interestingly, in several systems, PDF-family neuropeptides and/or the neurons that release them can modulate arousal and sensitivity to external stimuli [73–76]. Our results suggest that modulation of attention to sensory stimuli like ascr#3 could be an ancient function of this family of neuropeptides.

STAR METHODS

RESOURCE AVAILABLITY

Lead Contact

- Further information and requests for resources and reagents should be directed to and will be fulfilled by the Lead Contact, Douglas Portman (douglas.portman@rochester.edu).

Materials Availability

- Plasmids and nematode strains generated in the course of this work are freely available to interested academic researchers through the Lead Contact.

Data and Code Availability

- Source data obtained in the current study have not been deposited in a public repository but are available from the Lead Contact on request.
- This study did not generate code.
- Any additional information required to reanalyze the data reported in this work paper is available from the Lead Contact upon request.

EXPERIMENTAL MODEL AND SUBJECT DETAILS

All *C. elegans* strains were cultured using *E. coli* OP50 and NGM agar as described[77,78]. All strains were grown at 20°C except for those containing *daf-7* mutations; these were cultured

at 15°C from egg to L4 stage and then assayed at 20°C. *him-5(e1490)* is considered the wild-type for these studies. All strains used here contained this mutation unless otherwise noted.

METHOD DETAILS

Behavioral Assays

Quadrant assay with controlled bacterial thickness: Quadrant assays were performed as described previously [34] with the following modifications. To prepare lawns of controlled thicknesses, plates were seeded with bacterial cultures of defined concentration. To prepare these, 2 mL of *E. coli* OP50, freshly cultured in LB media, was collected and centrifuged (12,000 g for 30 sec). After determining its mass, the bacterial pellet was vigorously resuspended in sterile water (143 μL water for each 1 mg of *E. coli*) to create the T3 stock. T3 stock was diluted 0.1x to create T2 stock, which was then diluted 0.1x to create T1 stock. Each assay plate was seeded with 50 μL of stock suspension and incubated at 20°C for exactly 16 hr before t = 0 min. For three random T3 stocks, bacterial density was calculated by serial dilution to be 3.5×10^8, 8.8×10^8, and 2.8×10^9 cfu/mL. The variation among these samples is likely amplified by extensive serial dilution, as the lawns created with these stocks appeared identical under a stereomicroscope after 16 hours of incubation. We visually inspected lawn quality for each batch of plates before use and found this procedure to reliably produce lawns appearing like those in Figure 1B.

For each assay, 30 mins before t = 0 min, ten animals were picked to the center of each plate, with the experimenter blind to genotype. At t = 0, four 1 μL drops of ascr#3 or vehicle (an equivalent volume of ethanol diluted in sterile water) were dropped into each of the four quadrants. At t = 30, 60, 90, and 120 mins, the number of animals in each quadrant was scored. For each assay, the overall Quadrant Chemotaxis Index (QCI) was calculated as the mean of the four QCI values.

Foraging assay: On the day preceding the assay, L4 hermaphrodites were picked to OP50-seeded plates (30 animals per plate) and assay plates were prepared. Guided by a custom-made transparent template, the boundaries of a center square (“source patch”) and four peripheral rectangles (“outer patches”) were drawn on the bottom of each unseeded 10-cm NGM agar plate. The shape and size of the source patch is equivalent to a single quadrant in the quadrant assay. The shape and size of each outer patch is equivalent to two adjacent quadrants. The distance from the boundary of the source patch to the nearest boundary of an outer patch is 1.8 cm. T1 or T3 bacterial stocks were made as described above. For the source patch, 12.5 μL of T1 or T3 stock suspension was dropped and carefully spread. For each outer patch, 25 μL of T3 suspension was spread. All assay plates were then incubated at 20 °C for exactly 16 hr before t = 0.

At t = 0, 10 μL ascr#3 (1 μM solution) or vehicle control (ethanol diluted in sterile water) was dropped onto the source patch under the stereomicroscope. Air bubbles were created and quickly moved around on the square food lawn to cover it completely with the solution. Once the lawn was dry (3 to 5 min), 25 WT hermaphrodites (strain DR466) and 25 ASI-ablated hermaphrodites (strain UR1110) were picked into the source patch. Each plate was

incubated at 20°C for 3 hr. At t = 180 min, animals in the outer patches were counted and genotyped using GFP fluorescence.

Molecular biology and generation of transgenic strains—To express nCre in different cells, we created a series of nCre expression plasmids. Promoters were designed from sequence information from Wormbase and were amplified from purified *C. elegans* genomic DNA using Phusion DNA polymerase (New England Biolabs). nCre expression constructs containing these promoters and the *unc-54* 3'UTR were created using Gateway cloning (Thermo Fisher Scientific). All constructs were confirmed by Sanger sequencing. See Table S1 for primer sequences.

To create conditional *pdfr-1* rescue strains, the nCre expression plasmid was first injected into the strain UR930 with the co-injection marker Pvha-6::mCherry(mini), a gift from K. Nehrke. The resulting transgene was then crossed into the *kyEx4648* background (CX14488, generously provided by S. Flavell and C. Bargmann [41]) and maintained by picking hermaphrodites with both intestinal and pharyngeal mCherry signals.

All new extrachromosomal array transgenes were created by microinjection of DNA of interest at 20 ng/μL together with co-injection marker at 50 ng/μL. At least two lines were assayed for each new array. Genetic ablation strains were confirmed by DiI staining (for ablation of ADL, ASK, and ASI) or using a fluorescent marker (for ablation of ADF). Strains were genotyped by PCR and/or Sanger sequencing (see Table S2 for details).

QUANTIFICATION AND STATISTICAL ANALYSIS

Unless otherwise indicated, statistical significance was assessed using a two-tailed Mann-Whitney t-test with unequal variances (to compare two genotypes) or Tukey's multiple comparison test (to compare more than two genotypes) post one-way or two-way ANOVA, corresponding to the number of factors. Asterisks indicate p values associated with these tests: *$p \leq 0.05$; **$p \leq 0.005$; ***$p \leq 0.001$. For clarity, the brackets in each graph indicate all comparisons made; those with a statistically non-significant result ($p > 0.05$) are shown with dashed gray lines. For each group tested in the quadrant assay, we also carried out a one-sample t-test to ask whether there was a significant aversive or attractive response to ascr#3 (*i.e.*, to ask whether the QCI was statistically different from zero). The resulting p values are indicated with circles above each violin plot: °$p \leq 0.05$; °°$p \leq 0.005$; °°°$p \leq 0.001$.

Supplementary Material

Refer to Web version on PubMed Central for supplementary material.

ACKNOWLEDGEMENTS

We thank current and past members of the Portman lab, the University of Rochester Invertebrate Biology Group, and the Western New York Worm Group for discussion and critical feedback. We are particularly grateful to E. DiLoreto and J. Srinivasan, as well as K. Kim and P. Sengupta, for communicating unpublished results, and to F. Schroeder for providing synthetic ascr#3. We thank S. Flavell, C. Bargmann, T. Hirotsu, D. Ferkey, and K. Nehrke for generously providing strains and reagents. Some strains used in this work were provided by the *Caenorhabditis* Genetics Center, which is funded by NIH Office of Research Infrastructure Programs (P40 OD010440). These studies were funded by NIH R01 GM130136 and R01 GM140415 to D.P.

REFERENCES

1. Charnov EL (1976). Optimal foraging, the marginal value theorem. Theor Popul Biol 9, 129–136. 10.1016/0040-5809(76)90040-x. [PubMed: 1273796]
2. Pyke GH (1984). Optimal Foraging Theory: A Critical Review. Annual Review of Ecology and Systematics 15, 523–575. 10.1146/annurev.es.15.110184.002515.
3. Calhoun AJ, and Hayden BY (2015). The foraging brain. Current Opinion in Behavioral Sciences 5, 24–31. 10.1016/j.cobeha.2015.07.003.
4. Frezal L, and Felix MA (2015). C. elegans outside the Petri dish. Elife 4. 10.7554/eLife.05849.
5. Milward K, Busch KE, Murphy RJ, de Bono M, and Olofsson B (2011). Neuronal and molecular substrates for optimal foraging in Caenorhabditis elegans. Proceedings of the National Academy of Sciences of the United States of America 108, 20672–20677. 10.1073/pnas.1106134109. [PubMed: 22135454]
6. Harvey SC (2009). Non-dauer larval dispersal in Caenorhabditis elegans. J Exp Zool B Mol Dev Evol 312B, 224–230. 10.1002/jez.b.21287. [PubMed: 19288538]
7. Shtonda BB, and Avery L (2006). Dietary choice behavior in Caenorhabditis elegans. The Journal of experimental biology 209, 89–102. 10.1242/jeb.01955. [PubMed: 16354781]
8. Ben Arous J, Laffont S, and Chatenay D (2009). Molecular and sensory basis of a food related two-state behavior in C. elegans. PloS one 4, e7584. 10.1371/journal.pone.0007584. [PubMed: 19851507]
9. Zhang Y, Lu H, and Bargmann C (2005). Pathogenic bacteria induce aversive olfactory learning in Caenorhabditis elegans. Nature 438, 179–184. [PubMed: 16281027]
10. Melo JA, and Ruvkun G (2012). Inactivation of conserved C. elegans genes engages pathogen- and xenobiotic-associated defenses. Cell 149, 452–466. 10.1016/j.cell.2012.02.050. [PubMed: 22500807]
11. Pradhan S, Quilez S, Homer K, and Hendricks M (2019). Environmental Programming of Adult Foraging Behavior in C. elegans. Current biology : CB 29, 2867–2879 e2864. 10.1016/j.cub.2019.07.045. [PubMed: 31422888]
12. Calhoun AJ, Tong A, Pokala N, Fitzpatrick JA, Sharpee TO, and Chalasani SH (2015). Neural Mechanisms for Evaluating Environmental Variability in Caenorhabditis elegans. Neuron 86, 428–441. 10.1016/j.neuron.2015.03.026. [PubMed: 25864633]
13. de Bono M, and Bargmann CI (1998). Natural variation in a neuropeptide Y receptor homolog modifies social behavior and food response in C. elegans. Cell 94, 679–689. [PubMed: 9741632]
14. Bendesky A, Tsunozaki M, Rockman MV, Kruglyak L, and Bargmann CI (2011). Catecholamine receptor polymorphisms affect decision-making in C. elegans. Nature 472, 313–318. 10.1038/nature09821. [PubMed: 21412235]
15. Greene JS, Dobosiewicz M, Butcher RA, McGrath PT, and Bargmann CI (2016). Regulatory changes in two chemoreceptor genes contribute to a Caenorhabditis elegans QTL for foraging behavior. Elife 5. 10.7554/eLife.21454.
16. Greene JS, Brown M, Dobosiewicz M, Ishida IG, Macosko EZ, Zhang X, Butcher RA, Cline DJ, McGrath PT, and Bargmann CI (2016). Balancing selection shapes density-dependent foraging behaviour. Nature 539, 254–258. 10.1038/nature19848. [PubMed: 27799655]
17. Gloria-Soria A, and Azevedo RB (2008). npr-1 Regulates foraging and dispersal strategies in Caenorhabditis elegans. Current biology : CB 18, 1694–1699. 10.1016/j.cub.2008.09.043. [PubMed: 18993077]
18. Lipton J, Kleemann G, Ghosh R, Lints R, and Emmons SW (2004). Mate searching in Caenorhabditis elegans: a genetic model for sex drive in a simple invertebrate. The Journal of neuroscience : the official journal of the Society for Neuroscience 24, 7427–7434. [PubMed: 15329389]
19. Barrios A, Ghosh R, Fang C, Emmons SW, and Barr MM (2012). PDF-1 neuropeptide signaling modulates a neural circuit for mate-searching behavior in C. elegans. Nature neuroscience 15, 1675–1682. 10.1038/nn.3253. [PubMed: 23143519]
20. Barrios A, Nurrish S, and Emmons SW (2008). Sensory regulation of C. elegans male mate-searching behavior. Current biology : CB 18, 1865–1871. [PubMed: 19062284]

21. Wexler LR, Miller RM, and Portman DS (2020). C. elegans Males Integrate Food Signals and Biological Sex to Modulate State-Dependent Chemosensation and Behavioral Prioritization. Current biology : CB. 10.1016/j.cub.2020.05.006.

22. Ryan DA, Miller RM, Lee K, Neal SJ, Fagan KA, Sengupta P, and Portman DS (2014). Sex, age, and hunger regulate behavioral prioritization through dynamic modulation of chemoreceptor expression. Current biology : CB 24, 2509–2517. 10.1016/j.cub.2014.09.032. [PubMed: 25438941]

23. Giraldeau L-A, and Caraco T (2000). Social foraging theory (Princeton University Press).

24. Scott E, Hudson A, Feist E, Calahorro F, Dillon J, de Freitas R, Wand M, Schoofs L, O'Connor V, and Holden-Dye L (2017). An oxytocin-dependent social interaction between larvae and adult C. elegans. Sci Rep 7, 10122. 10.1038/s41598-017-09350-7. [PubMed: 28860630]

25. Ding SS, Muhle LS, Brown AEX, Schumacher LJ, and Endres RG (2020). Comparison of solitary and collective foraging strategies of Caenorhabditis elegans in patchy food distributions. Philos Trans R Soc Lond B Biol Sci 375, 20190382. 10.1098/rstb.2019.0382. [PubMed: 32713303]

26. Dal Bello M, Perez-Escudero A, Schroeder FC, and Gore J (2021). Inversion of pheromone preference optimizes foraging in C. elegans. Elife 10. 10.7554/eLife.58144.

27. Felix MA, and Duveau F (2012). Population dynamics and habitat sharing of natural populations of Caenorhabditis elegans and C. briggsae. BMC biology 10, 59. 10.1186/1741-7007-10-59. [PubMed: 22731941]

28. Ludewig AH, and Schroeder FC (2013). Ascaroside signaling in C. elegans. WormBook : the online review of C. elegans biology, 1–22. 10.1895/wormbook.1.155.1.

29. Park JY, Joo HJ, Park S, and Paik YK (2019). Ascaroside Pheromones: Chemical Biology and Pleiotropic Neuronal Functions. Int J Mol Sci 20. 10.3390/ijms20163898.

30. McGrath PT, and Ruvinsky I (2019). A primer on pheromone signaling in Caenorhabditis elegans for systems biologists. Curr Opin Syst Biol 13, 23–30. 10.1016/j.coisb.2018.08.012. [PubMed: 30984890]

31. Butcher RA, Fujita M, Schroeder FC, and Clardy J (2007). Small-molecule pheromones that control dauer development in Caenorhabditis elegans. Nature chemical biology 3, 420–422. 10.1038/nchembio.2007.3. [PubMed: 17558398]

32. Kim K, Sato K, Shibuya M, Zeiger DM, Butcher RA, Ragains JR, Clardy J, Touhara K, and Sengupta P (2009). Two chemoreceptors mediate developmental effects of dauer pheromone in C. elegans. Science 326, 994–998. 10.1126/science.1176331. [PubMed: 19797623]

33. Srinivasan J, Kaplan F, Ajredini R, Zachariah C, Alborn H, Teal P, Malik R, Edison A, Sternberg P, and Schroeder F (2008). A blend of small molecules regulates both mating and development in Caenorhabditis elegans. Nature 454, 1115–1118. 10.1038/nature07168. [PubMed: 18650807]

34. Fagan KA, Luo J, Lagoy RC, Schroeder FC, Albrecht DR, and Portman DS (2018). A Single-Neuron Chemosensory Switch Determines the Valence of a Sexually Dimorphic Sensory Behavior. Current biology : CB 28, 902–914 e905. 10.1016/j.cub.2018.02.029. [PubMed: 29526590]

35. Jang H, Kim K, Neal SJ, Macosko E, Kim D, Butcher RA, Zeiger DM, Bargmann CI, and Sengupta P (2012). Neuromodulatory state and sex specify alternative behaviors through antagonistic synaptic pathways in C. elegans. Neuron 75, 585–592. 10.1016/j.neuron.2012.06.034. [PubMed: 22920251]

36. Macosko EZ, Pokala N, Feinberg EH, Chalasani SH, Butcher RA, Clardy J, and Bargmann CI (2009). A hub-and-spoke circuit drives pheromone attraction and social behaviour in C. elegans. Nature 458, 1171–1175. 10.1038/nature07886. [PubMed: 19349961]

37. Fenk LA, and de Bono M (2017). Memory of recent oxygen experience switches pheromone valence in Caenorhabditis elegans. Proceedings of the National Academy of Sciences of the United States of America 114, 4195–4200. 10.1073/pnas.1618934114. [PubMed: 28373553]

38. Hong M, Ryu L, Ow MC, Kim J, Je AR, Chinta S, Huh YH, Lee KJ, Butcher RA, Choi H, et al. (2017). Early Pheromone Experience Modifies a Synaptic Activity to Influence Adult Pheromone Responses of C. elegans. Current biology : CB 27, 3168–3177 e3163. 10.1016/j.cub.2017.08.068. [PubMed: 28988862]

39. Ryu L, Cheon Y, Huh YH, Pyo S, Chinta S, Choi H, Butcher RA, and Kim K (2018). Feeding state regulates pheromone-mediated avoidance behavior via the insulin signaling pathway in

Caenorhabditis elegans. The EMBO journal 37, e98402. 10.15252/embj.201798402. [PubMed: 29925517]

40. Janssen T, Husson SJ, Lindemans M, Mertens I, Rademakers S, Ver Donck K, Geysen J, Jansen G, and Schoofs L (2008). Functional characterization of three G protein-coupled receptors for pigment dispersing factors in Caenorhabditis elegans. J Biol Chem 283, 15241–15249. 10.1074/jbc.M709060200. [PubMed: 18390545]
41. Flavell SW, Pokala N, Macosko EZ, Albrecht DR, Larsch J, and Bargmann CI (2013). Serotonin and the neuropeptide PDF initiate and extend opposing behavioral states in C. elegans. Cell 154, 1023–1035. 10.1016/j.cell.2013.08.001. [PubMed: 23972393]
42. Pungaliya C, Srinivasan J, Fox BW, Malik RU, Ludewig AH, Sternberg PW, and Schroeder FC (2009). A shortcut to identifying small molecule signals that regulate behavior and development in Caenorhabditis elegans. Proceedings of the National Academy of Sciences of the United States of America 106, 7708–7713. 10.1073/pnas.0811918106. [PubMed: 19346493]
43. Srinivasan J, von Reuss SH, Bose N, Zaslaver A, Mahanti P, Ho MC, O'Doherty OG, Edison AS, Sternberg PW, and Schroeder FC (2012). A modular library of small molecule signals regulates social behaviors in Caenorhabditis elegans. PLoS biology 10, e1001237. 10.1371/journal.pbio.1001237. [PubMed: 22253572]
44. Bargmann CI, and Horvitz HR (1991). Control of larval development by chemosensory neurons in Caenorhabditis elegans. Science 251, 1243–1246. [PubMed: 2006412]
45. McGrath PT, Xu Y, Ailion M, Garrison JL, Butcher RA, and Bargmann CI (2011). Parallel evolution of domesticated Caenorhabditis species targets pheromone receptor genes. Nature 477, 321–325. 10.1038/nature10378. [PubMed: 21849976]
46. Ren P, Lim CS, Johnsen R, Albert PS, Pilgrim D, and Riddle DL (1996). Control of C. elegans larval development by neuronal expression of a TGF-beta homolog. Science 274, 1389–1391. [PubMed: 8910282]
47. Schackwitz WS, Inoue T, and Thomas JH (1996). Chemosensory neurons function in parallel to mediate a pheromone response in C. elegans. Neuron 17, 719–728. [PubMed: 8893028]
48. Taylor SR, Santpere G, Weinreb A, Barrett A, Reilly MB, Xu C, Varol E, Oikonomou P, Glenwinkel L, McWhirter R, et al. (2021). Molecular topography of an entire nervous system. Cell. 10.1016/j.cell.2021.06.023.
49. Mehra A, Gaudet J, Heck L, Kuwabara PE, and Spence AM (1999). Negative regulation of male development in Caenorhabditis elegans by a protein-protein interaction between TRA-2A and FEM-3. Genes Dev 13, 1453–1463. [PubMed: 10364161]
50. Mowrey WR, Bennett JR, and Portman DS (2014). Distributed Effects of Biological Sex Define Sex-Typical Motor Behavior in Caenorhabditis elegans. The Journal of neuroscience : the official journal of the Society for Neuroscience 34, 1579–1591. 10.1523/JNEUROSCI.4352-13.2014. [PubMed: 24478342]
51. Lee K, and Portman D (2007). Neural sex modifies the function of a C. elegans sensory circuit. Current biology : CB 17, 1858–1863. 10.1016/j.cub.2007.10.015. [PubMed: 17964163]
52. White J, Nicholas T, Gritton J, Truong L, Davidson E, and Jorgensen E (2007). The sensory circuitry for sexual attraction in C. elegans males. Current biology : CB 17, 1847–1857. 10.1016/j.cub.2007.09.011. [PubMed: 17964166]
53. Herrero A, Romanowski A, Meelkop E, Caldart CS, Schoofs L, and Golombek DA (2015). Pigment-dispersing factor signaling in the circadian system of Caenorhabditis elegans. Genes Brain Behav 14, 493–501. 10.1111/gbb.12231. [PubMed: 26113231]
54. Meelkop E, Temmerman L, Janssen T, Suetens N, Beets I, Van Rompay L, Shanmugam N, Husson SJ, and Schoofs L (2012). PDF receptor signaling in Caenorhabditis elegans modulates locomotion and egg-laying. Molecular and cellular endocrinology 361, 232–240. 10.1016/j.mce.2012.05.001. [PubMed: 22579613]
55. O'Donnell MP, Chao PH, Kammenga JE, and Sengupta P (2018). Rictor/TORC2 mediates gut-to-brain signaling in the regulation of phenotypic plasticity in C. elegans. PLoS genetics 14, e1007213. 10.1371/journal.pgen.1007213. [PubMed: 29415022]
56. Janssen T, Husson SJ, Meelkop E, Temmerman L, Lindemans M, Verstraelen K, Rademakers S, Mertens I, Nitabach M, Jansen G, and Schoofs L (2009). Discovery and characterization of

a conserved pigment dispersing factor-like neuropeptide pathway in Caenorhabditis elegans. J Neurochem 111, 228–241. 10.1111/j.1471-4159.2009.06323.x. [PubMed: 19686386]

57. Entchev EV, Patel DS, Zhan M, Steele AJ, Lu H, and Ch'ng Q (2015). A gene-expression-based neural code for food abundance that modulates lifespan. Elife 4, e06259. 10.7554/eLife.06259. [PubMed: 25962853]
58. Dalfo D, Michaelson D, and Hubbard EJ (2012). Sensory regulation of the C. elegans germline through TGF-beta-dependent signaling in the niche. Current biology : CB 22, 712–719. 10.1016/j.cub.2012.02.064. [PubMed: 22483938]
59. Gallagher T, Kim J, Oldenbroek M, Kerr R, and You YJ (2013). ASI Regulates Satiety Quiescence in C. elegans. The Journal of neuroscience : the official journal of the Society for Neuroscience 33, 9716–9724. 10.1523/JNEUROSCI.4493-12.2013. [PubMed: 23739968]
60. Sawin ER, Ranganathan R, and Horvitz HR (2000). C. elegans locomotory rate is modulated by the environment through a dopaminergic pathway and by experience through a serotonergic pathway. Neuron 26, 619–631. [PubMed: 10896158]
61. Worthy SE, Haynes L, Chambers M, Bethune D, Kan E, Chung K, Ota R, Taylor CJ, and Glater EE (2018). Identification of attractive odorants released by preferred bacterial food found in the natural habitats of C. elegans. PloS one 13, e0201158. 10.1371/journal.pone.0201158. [PubMed: 30036396]
62. Witham E, Comunian C, Ratanpal H, Skora S, Zimmer M, and Srinivasan S (2016). C. elegans Body Cavity Neurons Are Homeostatic Sensors that Integrate Fluctuations in Oxygen Availability and Internal Nutrient Reserves. Cell Rep 14, 1641–1654. 10.1016/j.celrep.2016.01.052. [PubMed: 26876168]
63. Gray JM, Karow DS, Lu H, Chang AJ, Chang JS, Ellis RE, Marletta MA, and Bargmann CI (2004). Oxygen sensation and social feeding mediated by a C. elegans guanylate cyclase homologue. Nature 430, 317–322. [PubMed: 15220933]
64. Cheung BH, Cohen M, Rogers C, Albayram O, and de Bono M (2005). Experience-dependent modulation of C. elegans behavior by ambient oxygen. Current biology : CB 15, 905–917. [PubMed: 15916947]
65. Hallem EA, Spencer WC, McWhirter RD, Zeller G, Henz SR, Ratsch G, Miller DM 3rd, Horvitz HR, Sternberg PW, and Ringstad N (2011). Receptor-type guanylate cyclase is required for carbon dioxide sensation by Caenorhabditis elegans. Proceedings of the National Academy of Sciences of the United States of America 108, 254–259. 10.1073/pnas.1017354108. [PubMed: 21173231]
66. Hallem EA, and Sternberg PW (2008). Acute carbon dioxide avoidance in Caenorhabditis elegans. Proceedings of the National Academy of Sciences of the United States of America 105, 8038–8043. 10.1073/pnas.0707469105. [PubMed: 18524955]
67. Hilbert ZA, and Kim DH (2018). PDF-1 neuropeptide signaling regulates sexually dimorphic gene expression in shared sensory neurons of C. elegans. Elife 7, e36547. 10.7554/eLife.36547. [PubMed: 30024377]
68. Barrios A (2014). Exploratory decisions of the Caenorhabditis elegans male: a conflict of two drives. Seminars in cell & developmental biology 33, 10–17. 10.1016/j.semcdb.2014.06.003. [PubMed: 24970102]
69. Gruninger TR, Gualberto DG, and Garcia LR (2008). Sensory perception of food and insulin-like signals influence seizure susceptibility. PLoS genetics 4, e1000117. 10.1371/journal.pgen.1000117. [PubMed: 18604269]
70. Gruninger T, Gualberto D, LeBoeuf B, and Garcia L (2006). Integration of male mating and feeding behaviors in Caenorhabditis elegans. J Neurosci S 26, 169–179.
71. Marder E, O'Leary T, and Shruti S (2014). Neuromodulation of circuits with variable parameters: single neurons and small circuits reveal principles of state-dependent and robust neuromodulation. Annu Rev Neurosci 37, 329–346. 10.1146/annurev-neuro-071013-013958. [PubMed: 25032499]
72. Hobert O (2013). The neuronal genome of Caenorhabditis elegans. WormBook : the online review of C. elegans biology, 1–106. 10.1895/wormbook.1.161.1.
73. Ardiel EL, Yu AJ, Giles AC, and Rankin CH (2017). Habituation as an adaptive shift in response strategy mediated by neuropeptides. NPJ Sci Learn 2, 9. 10.1038/s41539-017-0011-8. [PubMed: 30631455]

74. Choi S, Chatzigeorgiou M, Taylor KP, Schafer WR, and Kaplan JM (2013). Analysis of NPR-1 Reveals a Circuit Mechanism for Behavioral Quiescence in C. elegans. Neuron 78, 869–880. 10.1016/j.neuron.2013.04.002. [PubMed: 23764289]

75. Fu Y, Tucciarone JM, Espinosa JS, Sheng N, Darcy DP, Nicoll RA, Huang ZJ, and Stryker MP (2014). A cortical circuit for gain control by behavioral state. Cell 156, 1139–1152. 10.1016/j.cell.2014.01.050. [PubMed: 24630718]

76. Dubowy C, and Sehgal A (2017). Circadian Rhythms and Sleep in Drosophila melanogaster. Genetics 205, 1373–1397. 10.1534/genetics.115.185157. [PubMed: 28360128]

77. Brenner S (1974). The genetics of *Caenorhabditis elegans*. Genetics 77, 71–94. [PubMed: 4366476]

78. Stiernagle T (2006). Maintenance of C. elegans. WormBook : the online review of C. elegans biology, 1–11. 10.1895/wormbook.1.101.1.

79. Beverly M, Anbil S, and Sengupta P (2011). Degeneracy and neuromodulation among thermosensory neurons contribute to robust thermosensory behaviors in Caenorhabditis elegans. The Journal of neuroscience : the official journal of the Society for Neuroscience 31, 11718–11727. 10.1523/JNEUROSCI.1098-11.2011. [PubMed: 21832201]

80. Hamakawa M, Uozumi T, Ueda N, Iino Y, and Hirotsu T (2015). A role for Ras in inhibiting circular foraging behavior as revealed by a new method for time and cell-specific RNAi. BMC biology 13, 6. 10.1186/s12915-015-0114-8. [PubMed: 25603799]

81. Krzyzanowski MC, Woldemariam S, Wood JF, Chaubey AH, Brueggemann C, Bowitch A, Bethke M, L'Etoile ND, and Ferkey DM (2016). Aversive Behavior in the Nematode C. elegans Is Modulated by cGMP and a Neuronal Gap Junction Network. PLoS genetics 12, e1006153. 10.1371/journal.pgen.1006153. [PubMed: 27459302]

82. Lopez-Cruz A, Sordillo A, Pokala N, Liu Q, McGrath PT, and Bargmann CI (2019). Parallel Multimodal Circuits Control an Innate Foraging Behavior. Neuron 102, 407–419 e408. 10.1016/j.neuron.2019.01.053. [PubMed: 30824353]

83. Allman E, Johnson D, and Nehrke K (2009). Loss of the apical V-ATPase a-subunit VHA-6 prevents acidification of the intestinal lumen during a rhythmic behavior in C. elegans. Am J Physiol Cell Physiol 297, C1071–1081. 10.1152/ajpcell.00284.2009. [PubMed: 19741196]

Highlights

- Abundant food blocks hermaphrodite avoidance of a key population density pheromone
- Food abundance is encoded by the conserved PDF/PDFR-1 neuropeptide system
- PDFR-1 acts in interneurons to modulate the salience of the aversive pheromone cue
- Food-pheromone integration allows value assessment and promotes adaptive foraging

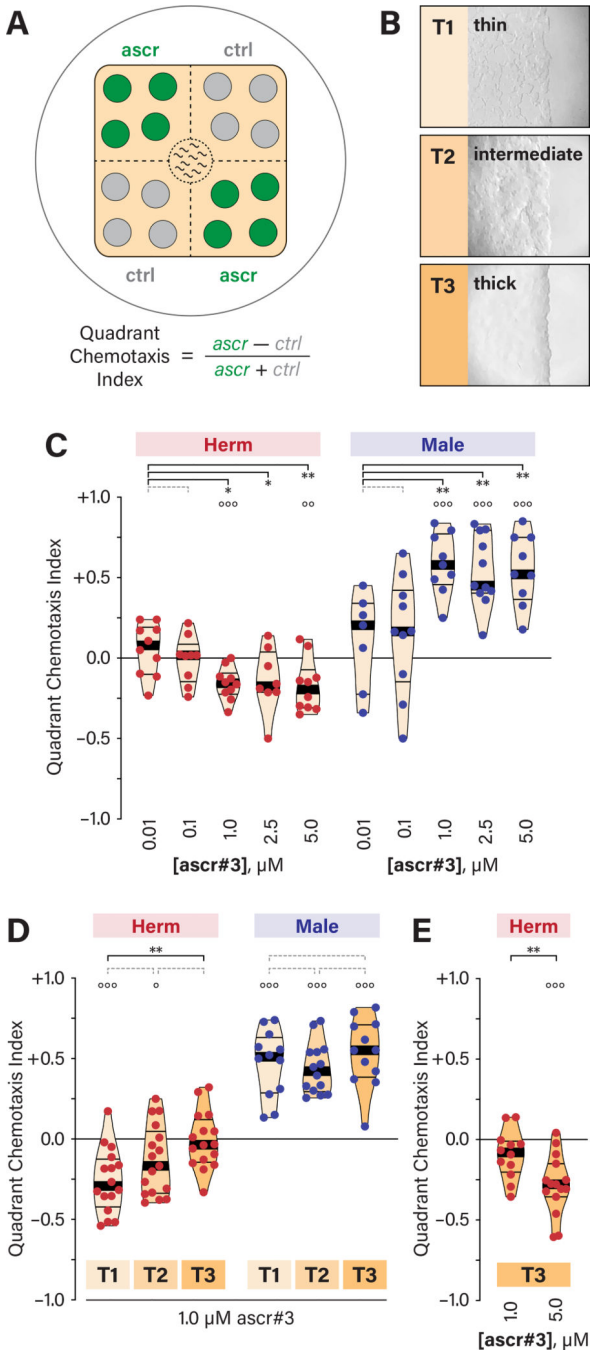

Figure 1. Hermaphrodite ascr#3 avoidance depends on food abundance.

(A) The quadrant-format behavioral assay [34]. **(B)** Images of representative bacterial lawns. T3, a thick lawn; T2, intermediate thickness; and T1, a sparse, patchy lawn. **(C)** Quadrant Chemotaxis Index (QCI) values for both sexes in response to a range of ascr#3 concentrations in the presence of thin food (T1). **(D)** QCIs for both sexes to 1.0 μM ascr#3 in three food conditions (T1, T2, and T3). **(E)** QCIs for adult hermaphrodites to 1.0 and 5.0 μM ascr#3 on thick food (T3). For all quadrant assay data shown in this and subsequent figures, data points are colored by sex (hermaphrodites, red; males, blue). Each point

represents a single assay containing 10 worms. Violin plots are shaded according to food thickness (T1, lighter; T3, darker). The median and interquartile intervals are indicated by thick and thin lines, respectively. Statistical comparisons are indicated with black brackets and asterisks (*$p \leq 0.05$; **$p \leq 0.005$; ***$p \leq 0.001$) or dotted gray brackets ($p > 0.05$). Open circles above each bar show the results of one-sample *t*-tests, indicating whether the observed QCI differs significantly from zero (°$p \leq 0.05$; °°$p \leq 0.005$; °°°$p \leq 0.001$). See also Figure S1.

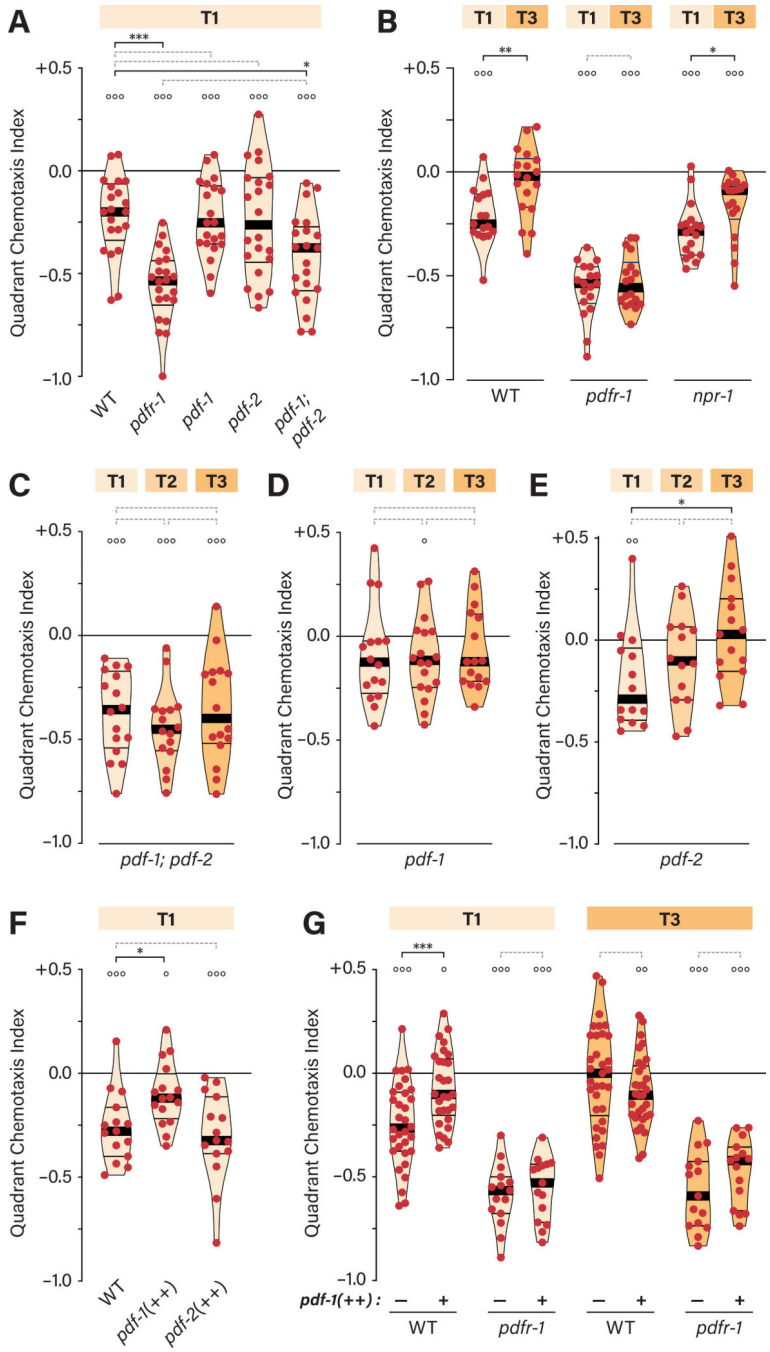

Figure 2. PDFR-1 signaling couples food abundance to ascr#3 avoidance.

(A) QCIs for WT, *pdfr-1*, *pdf-1*, *pdf-2*, and *pdf-1; pdf-2* hermaphrodites on T1. Unless otherwise noted (see Figure S2), all *pdfr-1* strains contain *pdfr-1(ok3425)*. **(B)** QCIs for WT, *pdfr-1*, and *npr-1* hermaphrodites on T1 and T3. **(C-E)** QCIs for *pdf-1*; *pdf-2* (C), *pdf-1* (D), and *pdf-2* (E) mutant hermaphrodites with the indicated food conditions. **(F)** QCIs for WT hermaphrodites and hermaphrodites overexpressing *pdf-1* (*pdf-1(++)*) and *pdf-2* (*pdf-2(++)*) on T1. **(G)** QCIs for WT, *pdf-1(++)*, *pdfr-1*, and *pdfr-1; pdf-1(++)* hermaphrodites on T1 and T3. See also Figure S2.

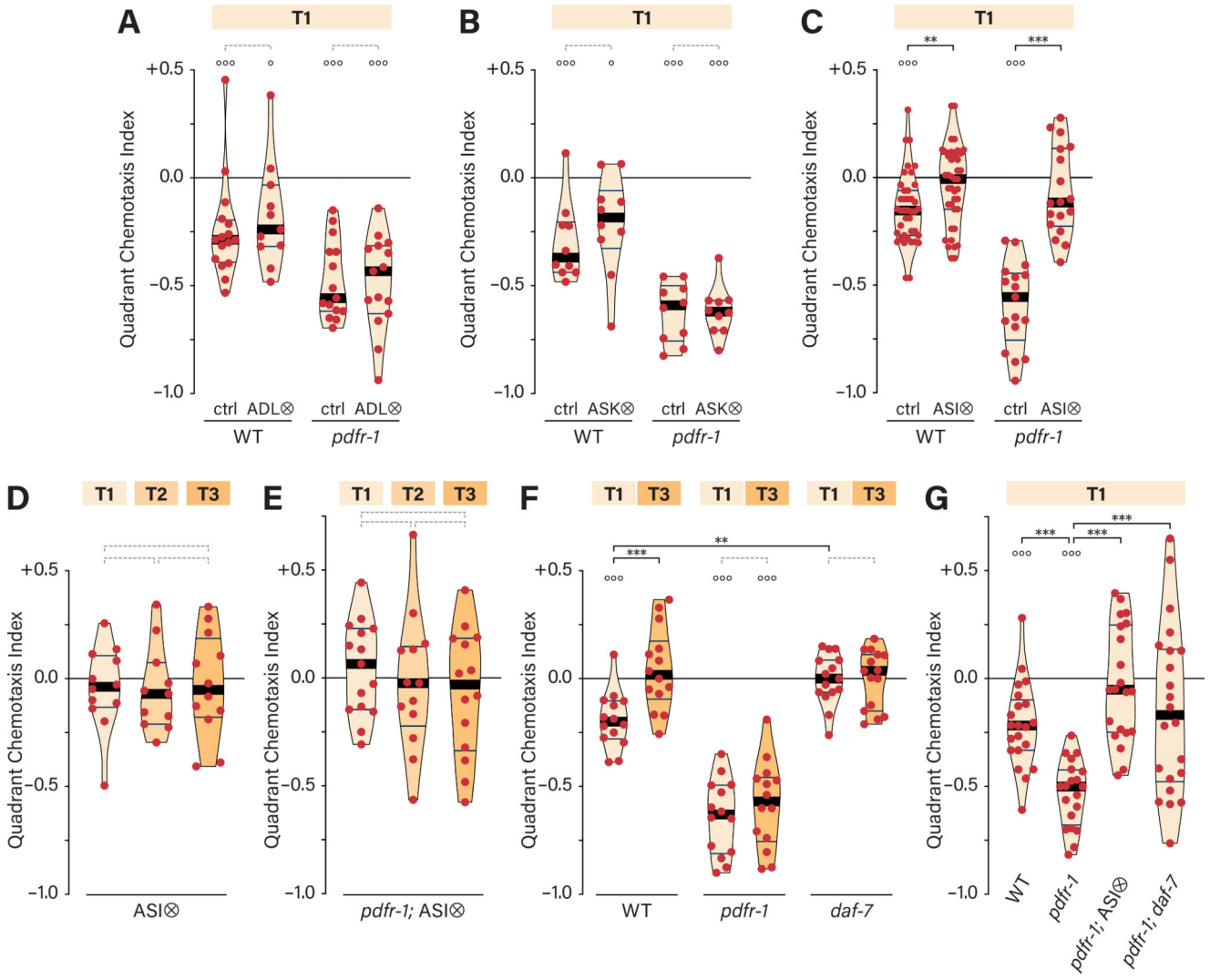

Figure 3. The ASI neurons mediate *pdfr-1*-dependent ascr#3 avoidance.

(A–C) QCIs for control and ADL-, ASK-, and ASI-ablated (ADL⊗, A; ASK⊗, B; ASI⊗, C) hermaphrodites in a wild-type or *pdfr-1* background on T1. **(D, E)** QCIs for ASI⊗ (D) or *pdfr-1*; ASI⊗ (E) hermaphrodites with three food conditions. **(F)** QCIs for WT, *pdfr-1*, and *daf-7* hermaphrodites with T1 and T3 food. **(G)** QCIs for WT, *pdfr-1*, *pdfr-1*; ASI⊗ and *pdfr-1; daf-7* hermaphrodites with T1 food. See also Figure S3.

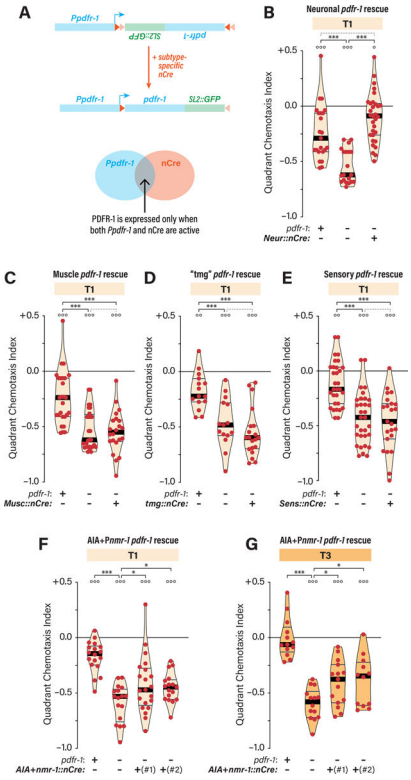

Figure 4. *pdfr-1* acts in a distributed set of interneurons to repress ascr#3 avoidance.

(A) The strategy for Cre-based conditional *pdfr-1* rescue [41]. **(B-G)** QCIs for hermaphrodites carrying a conditional *pdfr-1* transgene with the indicated *pdfr-1* genotypes (+, wild-type; −, mutant) without or with nCre transgenes expressed pan-neuronally ("*Neur::nCre*") (B), in muscle ("*Musc::nCre*") (C), in a set of interneurons where *pdfr-1* regulates motor state [41] ("*tmg::nCre*") (D), in sensory neurons ("*Sens::nCre*") (E), and in AIA and neurons expressing *nmr-1* ("*AIA+nmr-1::nCre*") (F, G), on T1 (B-F) or T3 (G) food.

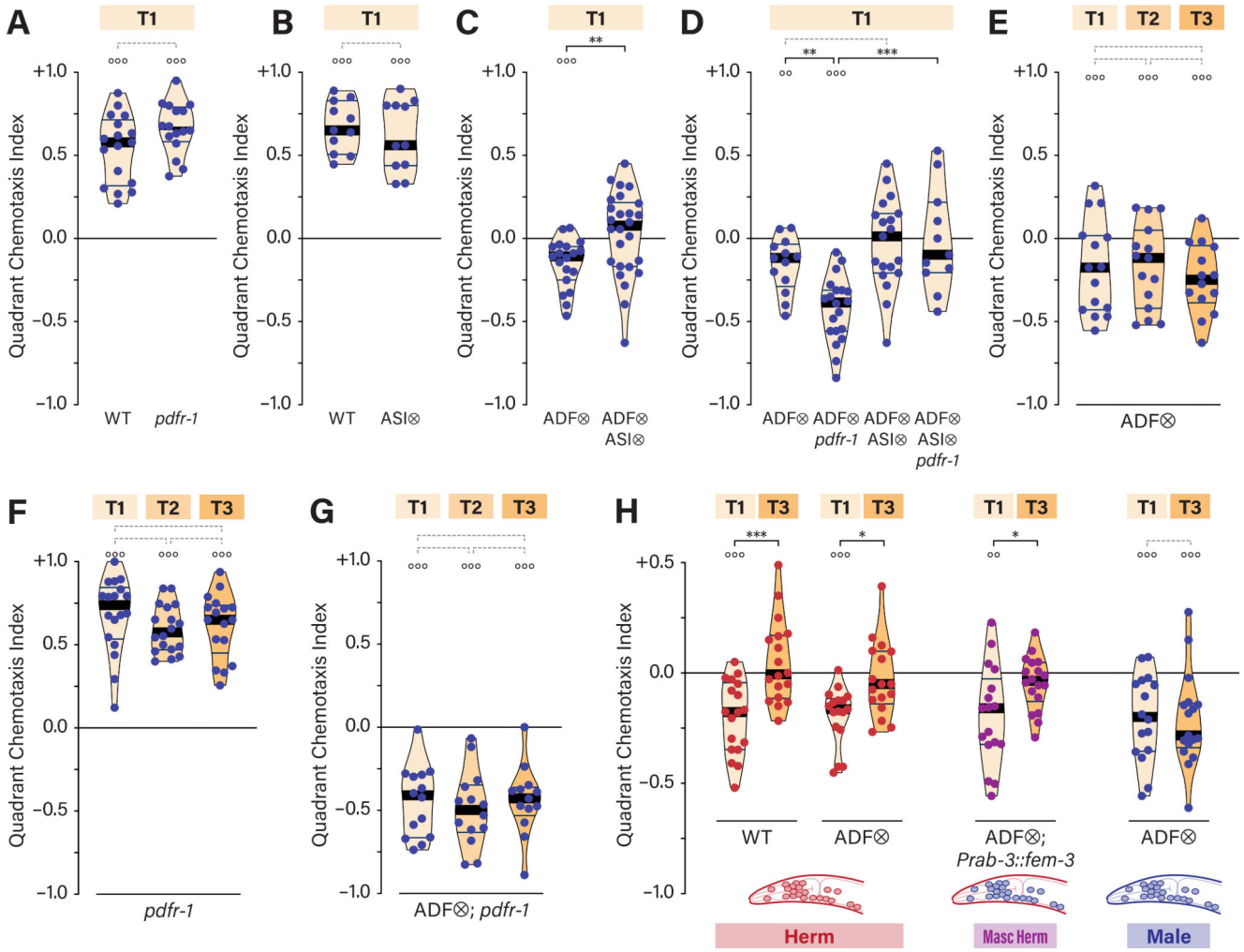

Figure 5. Latent ASI-dependent ascr#3 avoidance in males is independent of food abundance.

(A, B) QCIs for WT and *pdfr-1* (A) or ASI⊗ (B) males on T1 food. **(C)** QCIs for ADF⊗ and ADF⊗; ASI⊗ males on T1 food. **(D)** QCIs for ADF⊗, ADF⊗; *pdfr-1*, ADF⊗; ASI⊗, and *pdfr-1*; ADF⊗; ASI⊗ males on T1 food. **(E-G)** QCIs for ADF⊗ (E), *pdfr-1* (F), and ADF⊗; *pdfr-1* (G) with indicated food conditions. **(H)** QCIs for WT, ADF⊗, and ADF⊗; *Prab-3::fem-3* hermaphrodites and ADF⊗ males on T1 and T3 food.

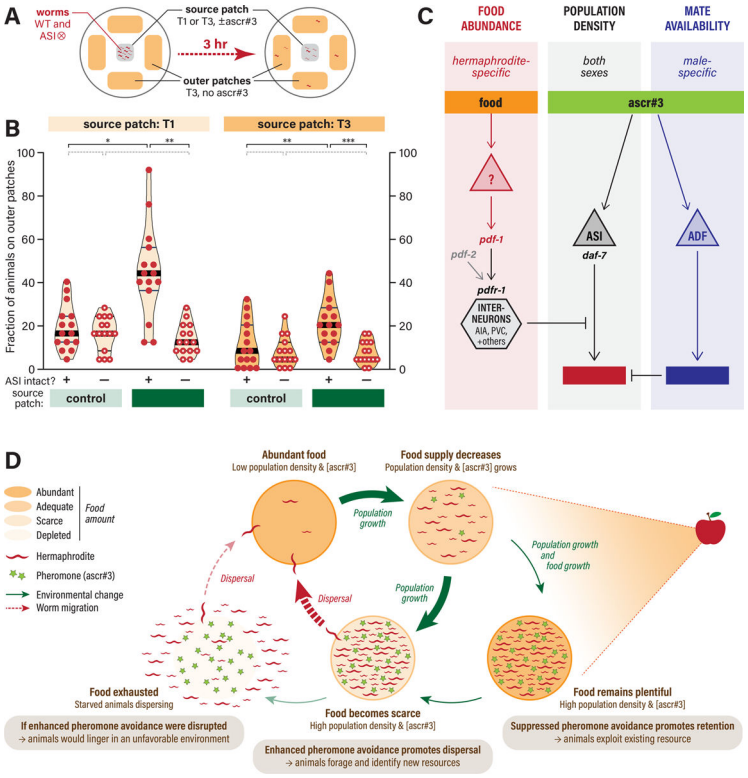

Figure 6. Modulation of ascr#3 aversion by food thickness enables flexibility in *C. elegans* foraging decisions.

(A) Experimental design. **(B)** Foraging rates, shown as the frequency of animals dispersing to the outer food sources, of WT and ASI⊗ hermaphrodites placed on a source patch of thick (T3) or thin (T1) food, without (−) or with (+) ascr#3. Each data point represents a single assay containing 25 worms per genotype. Filled and open circles indicate control and ASI-ablated animals, respectively. Violin plots are shaded according to food thickness at the source patch (T1, lighter; T3, darker). The median and interquartile intervals are indicated by thick and thin black lines, respectively. Statistical comparisons between groups are indicated with black brackets and asterisks (*$p \leq 0.05$; **$p \leq 0.005$; ***$p \leq 0.001$) or dotted gray brackets ($p > 0.05$). **(C)** A neural circuit model showing the parallel inputs of food abundance, ascr#3 via ASI, and ascr#3 via ADF. Hermaphrodite- and male-specific aspects are shown in red and blue, respectively. **(D)** A proposed model illustrating the adaptive value of context-dependent flexibility in *C. elegans* foraging behavior driven by modulation of ascr#3 avoidance.

KEY RESOURCES TABLE

REAGENT or RESOURCE	SOURCE	IDENTIFIER
Bacterial and Virus Strains		
E. coli OP50	CGC	OP50
Chemicals, peptides, and recombinant proteins		
ascaroside #3 (ascr#3, also known as C9 or asc-ΔC9)	Synthesized by F. Schroeder laboratory, Boyce Thomson Institute, Ithaca, NY	N/A
DiI (1,1′-Dioctadecyl-3,3,3′,3′-tetramethylindocarbocyanine perchlorate)	Sigma-Aldrich	Cat # 42364
Phusion HF DNA Polymerase	New England Biolabs	Cat # M0530L
Critical commercial assays		
MultiSite Gateway Three-Fragment Vector Construction Kit	Thermo Fisher Scientific	Cat # 12537-023
Experimental Models: Organisms/Strains		
him-5(e1490) V	CGC	DR466
C. elegans wild isolate	CGC	N2
npr-1(ky13) X	CGC [13]	CX4148
pdfr-1(ok3425) III	CGC	VC2609
pdfr-1(ok3425) III; him-5(e1490) V	This work (from DR466 and VC2609)	UR930
pdf-1(tm1996) III; him-5(e1490) V	This work (from DR466 and LSC27 [40])	UR954
him-5(e1490) V; pdf-2(tm4780) X	This work and [54]	UR955
lstEx2[pdf-1p::pdf-1::3′UTR + elt-2p::GFP]	CGC and [40]	LSC84
lstEx3[pdf-2p::pdf-2::3′UTR + elt-2p::GFP]	CGC and [40]	LSC54
daf-22(m130) II; him-5(e1490) V	This work (from DR466 and DR476, both from CGC)	UR978
pdfr-1(ok3425) III; him-5(e1490) V; kyEx4648[pdfr-1::inv[pdfr-1.d-sl2-GFP]]; fsEx595[rab-3p::Cre + vha-6p::mCherry #1]	This work and [41]	UR1363
pdfr-1(ok3425) III; him-5(e1490) V; kyEx4648[pdfr-1::inv[pdfr-1.d-sl2-GFP]]; fsEx596[rab-3p::Cre + vha-6p::mCherry #2]	This work and [41]	UR1364
pdfr-1(ok3425) III; him-5(e1490) V; kyEx4648[pdfr-1::inv[pdfr-1.d-sl2-GFP]]; fsEx597[myo-3p::Cre + vha-6p::mCherry #1]	This work and [41]	UR1365
pdfr-1(ok3425) III; him-5(e1490) V; kyEx4648[pdfr-1::inv[pdfr-1.d-sl2-GFP]]; fsEx598[myo-3p::Cre + vha-6p::mCherry #2]	This work and [41]	UR1366
pdfr-1(ok3425) III; him-5(e1490) V; kyEx4648[pdfr-1::inv[pdfr-1.d-sl2-GFP]]; fsEx599[nmr-1p::Cre + gcy-28d p::Cre + vha-6p::mCherry #1]	This work and [41]	UR1367
pdfr-1(ok3425) III; him-5(e1490) V; kyEx4648[pdfr-1::inv[pdfr-1.d-sl2-GFP]]; fsEx600[nmr-1p::Cre + gcy-28d p::Cre + vha-6p::mCherry #2]	This work and [41]	UR1368
pdfr-1(bx142) III; him-5(e1490) V	[19]	EM938
pdfr-1(ok3425) III; him-5(e1490) V; kyEx4648[pdfr-1::inv[pdfr-1.d-sl2-GFP]]; fsEx601[mod-1p::Cre +tdc-1p::Cre + glr-3::Cre + vha-6p::mCherry #1]	This work and [41]	UR1369
pdfr-1(ok3425) III; him-5(e1490) V; kyEx4648[pdfr-1::inv[pdfr-1.d-sl2-GFP]]; fsEx602[mod-1p::Cre +tdc-1p::Cre + glr-3::Cre + vha-6p::mCherry #2]	This work and [41]	UR1370

REAGENT or RESOURCE	SOURCE	IDENTIFIER
pdfr-1(ok3425) III; him-5(e1490) V; kyEx4648[pdfr-1::inv[pdfr-1.d-sl2-GFP]]; fsEx603[osm-6p::Cre + vha-6p::mCherry #1]	This work and [41]	UR1371
pdfr-1(ok3425) III; him-5(e1490) V; kyEx4648[pdfr-1::inv[pdfr-1.d-sl2-GFP]]; fsEx604[osm-6p::Cre + vha-6p::mCherry #2]	This work and [41]	UR1372
pdfr-1(ok3425) III; him-5(e1490) V; kyEx4648[pdfr-1::inv[pdfr-1.d-sl2-GFP]]; fsEx605[osm-6p::Cre+ mod-1::Cre + vha-6p::mCherry #1]	This work and [41]	UR1373
pdfr-1(ok3425) III; him-5(e1490) V; kyEx4648[pdfr-1::inv[pdfr-1.d-sl2-GFP]]; fsEx606[osm-6p::Cre+ mod-1::Cre + vha-6p::mCherry #2]	This work and [41]	UR1374
him-5(e1490) V; oyIs84[Pgpa-4::TU#813 + Pgcy-27::TU#814 + Pgcy-27::GFP + Punc-122::dsRed]	This work and [79] (from DR466 and PY7505)	UR1110
pdfr-1(ok3425) III; him-5(e1490) V; oyIs84[Pgpa-4::TU#813 + Pgcy-27::TU#814 + Pgcy-27::GFP + Punc-122::dsRed]	This work (from UR1110 and UR930)	UR1375
daf-7(e1372) III; him-5(e1490) V	This work	UR913
him-5(e1490) V; Ex[srh-281p::mCasp1 + myo-3p::GFP]	This work and T. Hirotsu [80]	UR1106
pdfr-1(ok3425) III; him-5(e1490) V; Ex[srh-281p::mCasp1 + myo-3p::GFP]	This work (from UR1106 and UR930)	UR1376
him-8(e1489) IV	CGC	CB1489
pdfr-1(ok3425) III; him-8(e1489) IV	This work (from CB1489 and VC2609)	UR1223
him-8(e1489) IV; qrIs2[sra-9::mCasp1] V	This work (from CB1489 and PS6025 (CGC))	UR1216
pdfr-1(ok3425) III; him-8(e1489) IV; qrIs2[sra-9::mCasp1] V	This work (from UR1223 and UR1216)	UR1231
daf-7(e1372) pdfr-1(ok3425) III; him-5(e1490) V	This work (from UR930 and UR913)	UR1378
him-5(e1490) V; udEx428[elt-2p::GFP + srh-142p::GFP + srh-142p::CED-3(p15) + srh-142p::CED-3(p17)]	This work and D. Ferkey [81]	UR987
him-5(e1490) fsIs15[rab-3p::FEM-3(+)::outron::mCherry + unc-122p::GFP] V; udEx428[elt-2p::GFP + srh-142p::GFP + srh-142p::CED-3(p15) + srh-142p::CED-3(p17)]	This work and D. Ferkey [22,81]	UR1379
pdfr-1(ok3425) III; him-5(e1490) V; udEx428[elt-2p::GFP + srh-142p::GFP + srh-142p::CED-3(p15) + srh-142p::CED-3(p17)]	This work (from UR930 and UR987)	UR1025
him-5(e1490) V; oyIs84[Pgpa-4::TU#813 + Pgcy-27::TU#814 + Pgcy-27::GFP + Punc-122::dsRed]; udEx428[elt-2p::GFP + srh-142p::GFP + srh-142p::CED-3(p15) + srh-142p::CED-3(p17)]	This work (from UR987 and UR1110)	UR1380
pdfr-1(ok3425) III; him-5(e1490) V; oyIs84[Pgpa-4::TU#813 + Pgcy-27::TU#814 + Pgcy-27::GFP + Punc-122::dsRed]; udEx428[elt-2p::GFP + srh-142p::GFP + srh-142p::CED-3(p15) + srh-142p::CED-3(p17)]	This work (from UR1025 and UR1375)	UR1381
pdf-1(tm1996) III; him-5(e1490) V; pdf-2(tm4780) X	This work (from UR954 and UR955)	UR1388
daf-22(m130) II; pdfr-1(ok3425) III; him-5(e1490) V	This work (from UR930 and UR978)	UR1389
him-5(e1490) V; lstEx2[pdf-1p::pdf-1::3′UTR + elt-2::GFP]	This work and [40] (from DR466 and LSC84)	UR1390
pdfr-1(ok3425) III; him-5(e1490) V; lstEx2[pdf-1p::pdf-1::3′UTR + elt-2::GFP]	This work and [40] (from UR1390 and UR930)	UR1391
Oligonucleotides		
See Table S1 for oligonucleotide information		
Recombinant DNA		
Prab-3::nCre	This work	N/A

REAGENT or RESOURCE	SOURCE	IDENTIFIER
Pmyo-3::nCre	This work	N/A
Pmod-1::nCre	This work	plasID_438
Ptdc-1::nCre	This work	N/A
Pglr-3::nCre	This work	N/A
Posm-6::nCre	This work	plasID_436
Pnmr-1::nCre	This work	N/A
Pgcy-28.d::nCre	C. Bargmann [82]	pALC07
Pvha-6::mCherry	K. Nehrke [83]	pELA1
Software and Algorithms		
ApE, A Plasmid Editor	M. Wayne Davis	N/A
Prism 8	GraphPad Software	N/A